Journal of Nuclear Medicine, published on June 21, 2017 as doi:10.2967/jnumed.116.185033

^{68}Ga-PSMA PET/CT and volumetric morphology of PET-positive lymph nodes stratified by tumor differentiation of prostate cancer

Maria Vinsensia[1], Peter L. Chyoke[2], Boris Hadaschik[3], Tim Holland-Letz[4], Jan Moltz[5], Klaus Kopka[6], Isabel Rauscher[7], Walter Mier[1], Markus Schwaiger[7], Uwe Haberkorn[1,8], Tobias Mauer[9], Clemens Kratochwil[1], Matthias Eiber[7,10] *, Frederik L. Giesel[1,8] *

1) Department of Nuclear Medicine, University Hospital Heidelberg, Germany
2) Molecular Imaging Program, National Institutes of Health, Bethesda, USA
3) Department of Urology, University Hospital Heidelberg, Germany
4) Department of Biostatistics, German Cancer Research Center (dkfz), Heidelberg, Germany
5) Fraunhofer MeVis, Bremen, Germany
6) Radiopharmaceutical Chemistry, German Cancer Research Center (dkfz), Heidelberg, Germany
7) Department of Nuclear Medicine, Klinikum Rechts der Isar, Technical University of Munich, Munich, Germany
8) Department of Molecular and Medical Pharmacology Cooperation Unit Nuclear Medicine, DKFZ Heidelberg, Germany
9) Department of Urology, TUM München, Klinikum rechts der Isar, Munich, Germnay
10) Department of Molecular and Medical Pharmacology, David Geffen School of Medicine at UCLA, Los Angeles, USA

*both authors contributed equally

Corresponding Author:
Frederik L. Giesel, M.D., M.B.A.
Vice Chair of Nuclear Medicine
Department of Nuclear Medicine, University Hospital Heidelberg
INF 400
69120 Heidelberg
Phone: +49-6221-56-39461
e-mail: frederik@egiesel.com

First Author:
Maria Vinsensia
Department of Nuclear Medicine, University Hospital Heidelberg
INF 400
69120 Heidelberg
Phone: +49-6221- 56-7732
e-mail: vinsensia@stud.uni-heidelberg.de

Word count: xxx

Short running title:
PSMA PET/CT lymph nodes prostate cancer

Abstract

^{68}Ga protate specific membrane antigene (PSMA) positron emission tomography (PET)/ computer tomography (CT) is a new method to detect early nodal metastases in patients with biochemical relapse of prostate cancer (PCa). In this retrospective investigation the dimensions, volume, localization and maximum standardized uptake value (SUV_{max}) of nodes identified by ^{68}Ga-PSMA were correlated to their Gleason score (GS) at diagnosis. Methods: All PET/CT images were acquired 60±10 min after intravenous injection of ^{68}Ga-PSMA (mean dose 176 MBq). In 147 prostate cancer patients (mean age 68; range 44-87 y) with prostate specific antigen (PSA) relapse (mean PSA level 5 ng/mL; range 0.25-294 ng/mL), 362 ^{68}Ga-PSMA PET positive lymph nodes (LN) were identified. These patients were classified based on their histopathology at primary diagnosis into either low (GS≤6, well-differentiated), intermediate (GS=7, moderately-differentiated) or high GS cohorts (GS≥8, poor-differentiated PCa). Using semi-automated LN segmentation software (MeVis, Bremen, GER), node volume, short and long axis dimensions (SAD, LAD) were measured based on CT and compared to the maximum standardized uptake value (SUV_{max}). Nodes demonstrating uptake of ^{68}Ga-PSMA with a SUV_{max}≥2.0 were considered PSMA-positive and nodes with SAD≥8 mm were considered positive by morphologic criteria. Results: Mean SUV_{max} was 13.5 (95% CI 10.9-16.1), 12.4 (95% CI 9.9-14.9) and 17.8 (95% CI 15.4-20.3) within the low, intermediate and high GS, respectively. The morphologic assessment of the ^{68}Ga-PSMA-positive LN demonstrated that the low GS cohort presented with smaller ^{68}Ga-PSMA positive LN (mean SAD 7.7 mm; n=113) followed by intermediate (mean SAD 9.4 mm; n=122) and high GS cohorts (mean SAD 9.5 mm; n=127). Based on the CT morphology criteria, only 34% of low GS patients, 56% of intermediate GS patients and 53% of high GS patients were considered CT positive. Overall, ^{68}Ga-PSMA imaging led to a reclassification of stage in 90 patients (61%) from cN0 to cN1 over CT. Conclusion: ^{68}Ga-PSMA PET is a promising modality in biochemical recurrent prostate cancer patients for N-staging. Conventional imaging underestimates lymph-node involvement compared to PSMA-molecular staging score in each GS cohort. The sensitivity

of ^{68}Ga-PSMA-PET/CT enables earlier detection of subcentimeter lymph node metastases in the biochemical recurrence setting.

Keywords:

PSMA-PET/CT, Morphology, N-Staging, lymph node, Prostate Cancer

Abstract word count: xxx (max 350)

Introduction

Biochemical recurrence (BCR) of PCa after initial therapy can herald an aggressive disease course. About one in three PCa patients who underwent local treatment with curative intent develops PSA-recurrence within 15 years *(1,2)*. PSA is a highly sensitive method for detecting recurrence and treatment of BCR is critical to prolong survival *(3)*. However, recurrences can occur in a variety of locations including the lymphatic tissue (30.5%), skeleton (42.1%), retroperitoneum (13.7%) and viscera (13.7%) *(4)*. Treatment varies according to the number and site of recurrence, but localizing such recurrences has been problematic with existing imaging methods such as computed tomography (CT) and bone scan due to their lack of sensitivity and specificity. For instance, only 11-14% of patients with biochemical failure after radical prostatectomy (RP) have positive CT scans *(5,6)* with similar results with MRI *(6-8)*. Therefore, detecting and localizing sites of recurrence is a strong unmet need for personalizing salvage therapy within individual patient.

Although a variety of positron emission tomography (PET) agents have been developed to detect prostate cancer recurrences, the most successful to date have been small molecule agents targeting prostate-specific membrane antigen (PSMA) *(9,10)*. One such agent, Glu-urea-Lys-(Ahx)-(^{68}Ga(HBED-CC)), also known as ^{68}Ga-PSMA, is particularly promising *(10-12).* ^{68}Ga-PSMA PET imaging has been shown to improve detection of lymph node metastasis and other sites of recurrence with very high positive predictive values and accuracy *(10,13,14).* Even though PET has a lower intrinsic spatial resolution of 3-5 mm compared with the submillimeter resolution for CT and MRI, ^{68}Ga-PSMA PET imaging has successfully detected nodal recurrences in two-thirds of patients who would have been missed using conventional CT morphological criteria *(15).* ^{68}Ga-PSMA PET/CT specifically benefits from the power of molecular imaging to detect small sized, but high target expressing lesions. One recent study demonstrated that ^{68}Ga-PSMA PET can achieve a sensitivity, specificity and accuracy of 77.9%,

97.3% and 89.9% for N-staging in recurrent disease *(13).* A meta-analysis involving 16 ^{68}Ga-PSMA PET articles covering 1309 patients reported a summary sensitivity and specificity of 80% and 97% on a per-lesion analysis *(14).*

Until now, the majority of ^{68}Ga-PSMA PET imaging studies have focused on the occurrence of lymph node metastases without correlation to the risk profile of the patient at primary diagnosis. For instance, the performance of ^{68}Ga-PSMA PET studies in PCa patients with histopathological low-risk disease is still lacking. Thus, the aim of this study was to compare the profiles of ^{68}Ga-PSMA PET positive nodal metastases in patients with BCR according to PSMA uptake and CT on well, moderately and poor differentiated PCa at initial diagnosis.

Material and Methods

Patients

In this two-center retrospective investigation, we evaluated 362 PET-positive lymph nodes in 147 consecutive patients (median age 68 y, range 44-87 y) with biochemical recurrence of prostate cancer (median PSA 5 ng/mL; range 0.2-294 ng/mL). The analysis was based on institutional databases at the University of Heidelberg and the Technical University Munich, which was randomized to reach a relatively equal cohort size. Only patients who underwent previous prostatectomy without any other oncological disease were included in this study. Gleason scores were obtained according to the reports on prostatectomy specimen and due to restriction of data, low GS patient's grading was based on either prostatectomy specimen or biopsy. Out of 51 low GS patients, 32 GS's grading was based on prostatectomy specimen and 19 GS's grading on biopsy. Biochemical recurrence was defined as two sequential improstate-specific antigen (PSA) values ≥0.2 ng/ml following prostatectomy *(3).* Patient characteristics are shown in *Table 1*. Prior to prostatectomy the median PSA was 13 ng/ml (range 2-252

ng/mL). Patients were stratified by Gleason score (GS) as follows: low GS (Gleason score≤6, well-differentiated PCa), intermediate GS (Gleason score=7, moderately-differentiated PCa) or high GS cohort (Gleason score≥8, poor-differentiated PCa). All patients were enrolled under an investigational protocol that was approved by the investigational review board of both universities and was in accordance with the Helsinki Declaration (permit S-321/12 at the University of Heidelberg and 5665/13 at the Technical University Munich). Written informed consent for anonymized evaluation and publication of their data were obtained from all patients.

Image acquisition, PSMA PET analysis and volumetric CT histogram analysis

All PET/CT examinations were performed on a Biograph 6 PET/CT or a Biograph mCT scanner (Siemens Medical Solutions, Erlangen, Germany). Imaging was initiated 60 ± 10 minutes after i.v. injection of ^{68}Ga-PSMA at a median dose of 2-3 MBq/kg body weight. On the Biograph 6 PET/CT a CT (130 keV, 80 mAs; CareDose) without contrast medium was performed for attenuation correction of the PET scan. On the Biograph mCT first a diagnostic CT scan was performed in the portal venous phase 80 s after intravenous injection of contrast agent (Imeron 300, Bracco Imaging, Milan, Italy) followed by the PET scan.

Static emission scans, corrected for dead time, scatter and decay, were acquired from the vertex to the proximal legs—requiring eight bed positions, each taking 3-4 minutes. The images were iteratively reconstructed with an ordered subset expectation maximization algorithm using four iterations with eight subsets and Gaussian filtering with an in-plane spatial resolution of 5 mm at full-width half-maximum. For calculation of the standardized uptake value (SUV), circular regions of interest were drawn around the region of interest on transaxial slices and automatically adapted to a three-dimensional volume of interest with e.soft software (Siemens) at a 70% isocontour. The CT scan was reconstructed with a B30 kernel to a slice thickness of 5 mm with an increment of 2.5 mm.

The threshold SUV_{max} for discriminating between benign and malignant lymph nodes in ^{68}Ga-PSMA PET was based on a blood pool sample from 20 patients in each group and results from a recent prospective study in primary PCa evaluating the use of SUV-thresholding *(15,16).* Upon these considerations lymph nodes were considered abnormal if their uptake SUV exceeded 2.0. A maximum of 3 malignant nodes were identified in all patients. If a patient harbored more than 3 lymph nodes metastases, we chose three most prominent lymph nodes with highest SUV_{max} value as it represents PSMA uptake. All suspected lymph nodes were assigned to one of the following anatomic locations: regional lymph node metastasis including internal iliac, external iliac, obturator fossa, presacral and distant lymph node metastasis for those around common iliac, paraaortic, paracaval/interaortocaval and other regions e.g. cervical and mediastinal *(17).*

Volumetric CT analysis was performed on ^{68}Ga-PSMA PET-positive nodes using semi-automated software (Fraunhofer MEVIS) that segments the nodes and automatically determines mean density, short axis diameter (SAD), long axis diameter (LAD) and volume *(Figure 1 and 2)*. Semiautomatic 3D histogram analysis was performed after the user provided a seed point in the lymph node and the software found the margins of the node. The segmentation starts with a fixed-width thresholding around the seed point. To remove attached vessels, muscles or other lymph nodes, a watershed transform was performed on the distance map of the thresholding result. The watershed transform is controlled to include and exclude features which are set according to an ellipsoid approximation of the lymph node. Quantitative and qualitative data of each patient were analyzed by one experienced radiologist and one nuclear medicine physician in each center. The volumes were evaluated by a radiologist to ensure that no extra nodal tissue was segmented and each node were manually corrected in all three dimensions, if necessary. The inter- and intra-observer reproducibility demonstrated a coefficient of variation < 5% *(18).* Any lymph node with SAD above 8 mm was considered positive according to CT criteria *(7,8).* The

size, represented by volume, short and long axis diameters and node location was recorded for every node.

Statistical evaluation

The evaluation of each group was based on the following parameters: measured SUV_{max}, volume, short-axis diameter and long-axis diameter. To account for multiple observations within the same patients, (up to 3 lymph nodes) comparisons between different risk cohorts were performed using a linear mixed model with risk group as a fixed effect and patient ID as a random effect. Descriptive statistics defining the percentage of positive PET/CT scans with nodes smaller than the above size criteria were performed. Statistical calculations were performed using the software SAS (Proc Mixed, SAS Institute, Cary, NC) and IBM SPSS Statistics (IBM Corp., Armonk, NY).

Results

Among 147 patients with biochemical recurrence, a total of 362 positive lymph nodes were evaluated on [6figure] ^{8}Ga-PSMA-PET/CT. The mean SUV_{max} of ^{68}Ga-PSMA uptake in malignant nodes was 14.67 (Interquartile Range 11.0-17.0). One hundred thirteen lymph nodes in 51 low Gleason score patients, 122 lymph nodes in 48 intermediate GS patients and 127 lymph nodes in 48 high GS patients were positive on ^{68}Ga-PSMA PET scan. Median initial PSA (iPSA) in the low GS cohort was 11.3 ng/mL (range 3.2-84.3 ng/mL); in the intermediate GS cohort iPSA was 12.0 ng/mL (range 3.8-252.0 ng/mL) and in the high GS cohort iPSA was 23.5 ng/mL (range 2.0-241.0 ng/mL). Median PSA-values at imaging were 5.0 ng/mL (range 0.5-41.3 ng/mL); 5.1 ng/mL (range 0.3-212 ng/mL) and 5.0 ng/mL (range 0.2-293.7 ng/mL) for low, intermediate and high GS patients *(Table 1).*

^{68}Ga-PSMA ligand uptake

The ^{68}Ga-PSMA ligand uptake showed a non-significant difference between the three GS cohorts (p=0.062). Mean SUV_{max} of affected lymph nodes in low, intermediate and high GS cohort was 13.5 (95% confidence interval (CI) 10.9-16.1); 12.4 (95% CI 9.9-14.9) and 17.8 (95% CI 15.4-20.3), respectively *(Table 2, Figure 3a).* Although the p-value of uptake between the intermediate and high GS cohort was less than 0.05 (p=0.031), it is considered as non-significant because the p-value of mixed model of the three cohorts was ≥0.05 *(Table 3).*

Morphometric analyses

The 3D-volumetric segmentation enabled derivation of several important parameters: lymph node size represented by short and long-axis diameter and lymph node volume of ^{68}Ga-PSMA PET positive findings. The short-axis diameter (SAD) between GS cohorts demonstrated significant differences (p=0.013) as follows: mean low GS SAD 7.7 mm (95% CI 6.9-8.4 mm; n=113); intermediate GS

SAD 9.4 mm (95% CI 8.6-10.2 mm; n=122) and high GS SAD was 9.5 mm (95% CI 8.7-10.4 mm; n=127) *(Table 2, Figure 3b).* Pairwise comparisons for lymph node SADs showed a significant difference between low and intermediate GS cohorts (p=0.011) and low and high GS lymph node SADs (p=0.009) *(Table 3).* The difference in SAD between the intermediate and high GS cohort was not significant. ^{68}Ga-PSMA positive lymph nodes also showed differences in long-axis diameter (LAD) (p=0.023) according to GS cohort with a mean low GS LAD of 11.9 mm (95% CI 11.0-12.7 mm); intermediate GS mean LAD of 13.9 mm (95% CI 12.8-14.9 mm) and high GS LAD of 14.2 mm (95% CI 13.1-15.2 mm). However, as seen in *Table 3*, overall lymph node volumes were not significantly different among the 3 cohorts.

Among the 113 PSMA positive lymph nodes (found in 31 of 51 patients) in the low GS cohort, 75 (66%) were morphologically negative (≤8 mm) on CT and 38 (34%) were morphologically positive. In the intermediate GS cohort, among 122 PSMA positive lymph nodes, 53 (44%) were morphologically negative and 69 (56%) were morphologically positive. In the high GS group, among 127 consecutive PSMA positive lymph nodes, 60 (47%) nodes were morphologically negative and 67 (53%) were morphologically positive. *Figure 5* depicts the morphological distribution in each cohort next to the CT morphological cut-off line of 8 mm and 10 mm. Therefore, among 362 PSMA positive lymph nodes, 174 (48%) were positive based on conventional imaging criteria and 188 nodes (52%) were negative.

Staging results by imaging modality

For each risk cohort, ^{68}Ga-PSMA PET/CT imaging demonstrated superior tumor detection to CT. Using standard TNM-Staging CT would have properly staged only 57 (38%) of 147 patients. By this standard, 35 patients (69%) of the low GS cohort, 29 patients (60%) of the intermediate GS and 26 patients (54%) of high GS would falsely be considered as cN0 by CT criteria. Overall, ^{68}Ga-PSMA PET/CT led to reclassification of 90 patients (61%) from cN0 to cN1.

Location of lymph nodes

Among the nodes detected by ^{68}Ga-PSMA PET, 254 (70%) were located in distant lymphatic stations (common iliac vessel, paraaortic, paracaval/interaortocaval and other regions e.g. cervical and mediastinal), meanwhile 108 (30%) nodes were in regional, pelvic lymph node stations (internal iliac vessel, external iliac vessel, obturator fossa and presacral). Distant ^{68}Ga-PSMA PET/CT positive lymph nodes were found in 84% of low GS patients, 68% of intermediate GS patients and 71% of high GS patient. Regional nodes were found in 16%, 32% and 29% of low, intermediate and high GS cohorts respectively. The most common location for a distant malignant node was the paraaortic station (17%), followed by the interaortocaval region and mediastinal.

Discussion

In this study, we have shown that ^{68}Ga-PSMA PSMA-PET imaging is superior to conventional CT criteria independent of initial tumor differentiation of prostate cancer. ^{68}Ga-PSMA ligand uptake in patients with biochemical recurrence may vary according to the Gleason score of the patient. Multiple studies have shown that the sensitivity and specificity of ^{68}Ga-PSMA PET/CT varies from 54-94% and 97-100% *(10,12-15,19).* Due to ethical and practical reason histopathological verification could only be obtained in 4/147 patients who underwent salvage lymphadenectomy after ^{68}Ga-PSMA PET. In all other patients a comprehensive standard of reference including contrast enhanced-CT, MRI, repeated ^{68}Ga-PSMA ligand PET/CT and course of PSA confirming the initial suspicious lesion(s) or showing disappearance of suspected lesion(s) after local/systemic treatment was obtained also suggesting the malignancy nature of the detected nodes.

The ^{68}Ga-PSMA uptake increases with the initial risk profile of the patient. One potential confounder in this study would be other malignancies. Thyroid, colon, kidney and brain malignancies

have also shown PSMA uptake. Therefore, in this study we intentionally excluded patients with other oncological disease to avoid these false-positive findings. Other studies have also reported possible false positives in the cervical, coeliac and sacral ganglia *(20,21).* The SUV_{max} of ganglia however, were relatively low compared to actual lymph nodes metastasis. Moreover, the localization of positive PSMA uptake corresponded to well-known lymph node stations further lowering the possibility of a false positive.

A comparison of two main parameters, ^{68}Ga-PSMA PET SUV_{max} and SAD on CT is shown in *Figure 4*. The morphological distribution as shown in *Figure 5* illustrates that nodal staging with CT alone strongly underestimates nodal involvement. Only 48% of all ^{68}Ga-PSMA PET/CT positive nodes exceeded the size criteria for metastasis on CT. The CT sensitivity calculated in this study (48%) is consistent with the existing data published *(5,6).* In the low GS cohort most (66%) positive lymph nodes were smaller than 8 mm. Regardless of their small size, these nodes demonstrated excellent uptake with a mean of SUV_{max} 13.5 (95% CI 10.9-16.1). Though it is important for patient management to detect and localize the sites of recurrence as early as possible, cross-sectional imaging is known to be insufficient. Detecting the metastases while the lesions are still small may allow earlier and individually tailored salvage therapies *(3,22).*

Prostate cancer patients with low initial Gleason score are considered unlikely to recur but nonetheless do probably because of higher grade disease that is not diagnosed at biopsy. This is also one limitation of our study: 19/51 gradings were done by biopsy which might translate into some “understaging” by sampling error in comparison to histological work-up of whole gland after prostatectomy. It is unclear whether PSMA-PET on biochemical relapse is as useful in these low GS patients as it is in higher GS patients who have a known likelihood of progression. Patients with local recurrence in the low risk group typically respond very well to early salvage radiotherapy *(23).* Therefore, the findings of this study might offer the possibility to further individualize salvage-radiation and to

possibly use targeted radiotherapy to recurrent lesions in the future, thus sparing unnecessary pelvic irradiation. We identified pelvic LN-metastases in 61% of BCR patients with initial low-risk GS, which is well in line with recent literature who reported LN-metastases as reason for BCR in 81% of patients using response to salvage radiotherapy as standard of reference (*24*).

The localization of the nodal involvement is also essential to determine whether systemic or regional salvage treatments are required. ^{68}Ga-PSMA PET/CT imaging provides indispensable information about the location and number of metastasis. In fact, because most patients had previous pelvic lymph node resections, most of the positive nodes (70%) in this study were located in more distant lymph stations. Thus, this kind of information could have a significant impact on potential radiation therapy planning similar to the results recently reported by van Leeuwen et al *(25).*

Comparison of the three GS groups showed significant differences in the diameters (SAD and LAD) of detected nodes according to risk cohort. Although SAD and LAD should correlate with the volume, nodal volume did not correlate well with risk correlation. It is possible that shape (reflected better as SAD and LAD) plays a more important role than volume per se. It is also possible that the software over- or underestimates volume whereas diameter determination is more readily verified. Furthermore, these results may also be an artifact of selecting only the 3 most prominent nodes in men with multiple metastases. The time interval of biochemical recurrence corresponds with the risk profile of each cohort. BCR tends to occur on low GS patients within the longest time interval of 103 months, meanwhile on intermediate and high GS patients BCR occurred within 56 months and 45 months, respectively. On such cases, the BCR-free interval and SAD of lymph node metastases may indicate the tissue growth/malignancy of the metastases in each cohort. However, more research is needed to better understand the correlation between time interval and the malignancy of the metastases.

Our results are similar to previous studies. A ^{68}Ga-PSMA study of 53 positive lymph nodes in intermediate and high risk patients (Gleason score ≥7) showed an SUVmax of 12.7 (range 2.4-51.0) with a corresponding node size of 8.3 mm (range 4-25 mm) *(13).* These data are in line with our evaluation of intermediate and high risk cohorts. In comparison the mean SUV_{max} in this study was 12.4 (range 2-49) and the SAD was 9.4 mm (range 1.9-33.5 mm) in the intermediate risk group and mean SUVmax 17.8 (range 2-97) and SAD of 9.5 mm (range 2.6-29.1 mm) in the high risk cohort.

The classification of the subgroups in this study was based on the Gleason score. The Gleason score was determined at the initial PCa diagnosis, thus making its relevance in a recurrence/relapse situation questionable since the patient has received prostatectomy and/or other therapy. However, the correlation of Gleason score and the risk of recurrent prostate cancer has been reported in various studies. The guidelines on prostate cancer published by the European Association of Urology, for instance, uses the classification of Gleason score (at biopsy) as a predictor of biochemical relapse *(3).* However, there has been some modifications regarding the definition of Gleason score 6, which upgraded the previous classification of Gleason 6 into Gleason 7a *(26).* Some patients in this study were diagnosed before 2010, thus the Gleason grading reported may not be equal with the current definition. Overall, using the Gleason score makes our results more generalizable.

Despite the retrospective nature of this study, randomized patient selection within each GS cohort and blinded analysis might help in reducing unforeseen biases. The selection of the 3 most prominent ^{68}Ga-PSMA positive lymph nodes from each patient might tend to overestimate the SUV_{max} value and lesions volumes of each group, but at the same time reduce the in-patient uptake bias. The lack of routine histological validation is one limitation of this study; however after BCR surgery is rarely an option and clinical follow-up or imaging are routinely used standards of reference in this setting.

^{68}Ga-PSMA PET/CT is promising as a better re-staging modality for prostate cancer patient with PSA relapse. A further investigation with a better differentiation of the recurrence subgroup could provide a more refined indication of the size and SUV_{max} of lymph nodes as a function of assigned risk stratification. Beside Gleason score, other relevant parameters such as PSA-doubling time, tumor invasion specify (pT-Stadium) and time to PSA-recurrence are intriguing and could provide a better specification for patient management. However, further new F18-labelled PSMA-ligands recently published allows higher patients throughput and also will guarantee PSMA-Diagnostics in to the uro-oncological environment on a daily basis for both T- and N-/M-Staging *(27,28,29)*.

Conclusion

This retrospective study demonstrates that ^{68}Ga-PSMA PET imaging is clearly superior to CT for detecting recurrent nodal disease independently of initial histology. Within risk strata established at diagnosis there are subtle differences both in uptake and node diameters according to initial Gleason scores. The ability of ^{68}Ga-PSMA PET/CT to better stage recurrent disease along with its ability to pinpoint metastatic sites makes it a valuable tool in assessing patients with BCR regardless of the initial risk cohort.

Disclosure

There is no potential conflict of interest relevant to this article.

Acknowledgments

None.

References

1. Moschini M, Sharma V, Zattoni F, et al. Natural history of clinical recurrence patterns of lymph node-positive prostate cancer after radical prostatectomy. *Eur Urol.* 2016;69:135-42.

2. Freedland SJ, Presti JC Jr, Amling CL, et al. Time trends in biochemical recurrence after radical prostatectomy: results of the SEARCH database. *Urology.* 2003;61:736-41.

3. N. Mottet, J. Bellmunt, E. Briers, et al. Guidelines on prostate cancer. *European Association of Urology*. 2015:80-84.

4. Nini A, Gandaglia G, Fossati N, et al. Patterns of clinical recurrence of node-positive prostate cancer and impact on long-term survival. *Eur Urol.* 2015;68:777-84.

5. Engeler CE, Wasserman NF, Zhang G. Preoperative assessment of prostatic carcinoma by computerized tomography weaknesses and new perspectives. *Urology.* 1992;40:346-50.

6. Hövels AM, Heesakkers RA, Adang EM, et al. The diagnostic accuracy of CT and MRI in the staging of pelvic lymph nodes in patients with prostate cancer: a meta-analysis. *Clin Radiol.* 2008;63:387-95.

7. Park SY, Oh YT, Jung DC, et al. Prediction of micrometastasis (<1 cm) to pelvic lymph nodes in prostate cancer: role of preoperative MRI. *AJR Am J Roentgenol.* 2015;205:328-34.

8. McMahon CJ, Rofsky NM, Pedrosa I. Lymphatic metastases from pelvic tumors: anatomic classification, characterization and staging. *Radiology.* 2010;254:31–46.

9. Eder M, Eisenhut M, Babich J, et al. PSMA as a target for radiolabelled small molecules. *Eur J Nuc Med Mol Imaging.* 2013;40:819-823.

10. Afshar-Oromieh A, Avtzi E, Giesel FL, et al. The diagnostic value of PET/CT imaging with the (68)Ga-labelled PSMA ligand HBED-CC in the diagnosis of recurrent prostate cancer. *Eur J Nucl Med Mol Imaging.* 2015;42:197-209.

11. Eder M, Schäfer M, Bauder-Wüst U, et al. ^{68}Ga-complex lipophilicity and the targeting property of a urea-based PSMA inhibitor for PET imaging. *Bioconjug Chem.* 2012;23:688-97.

12. Eiber M, Maurer T, Souvatzoglou M, et al. Evaluation of hybrid ^{68}Ga-PSMA ligand PET/CT in 248 patients with biochemical recurrence after radical prostatectomy. *J Nucl Med.* 2015;56:668-74.

13. Rauscher I, Maurer T, Beer AJ, et al. Value of ^{68}Ga-PSMA HBED-CC PET for the assessment of lymph node metastases in prostate cancer patients with biochemical recurrence: comparison with histopathology after salvage lymphadenectomy. *J Nucl Med.* 2016;57:1713-1719.

14. Perera M, Papa N, Christidis D, et al. Sensitivity, specificity, and predictors of positive ^{68}Ga-prostate-specific membrane antigen positron emission tomography in advanced prostate cancer: a systematic review and meta-analysis. *Eur Urol.* 2016;70:926-937.

15. Leeuwen PJ, Emmett L, Ho B, et al. Prospective evaluation of ^{68}Gallium-PSMA positron emission tomography/computerized tomography for preoperative lymph node staging in prostate cancer. *BJU Int.* 2017;119:209-215.

16. Giesel FL, Fiedler H, Stefanova M, et al. PSMA PET/CT with Glu-urea-Lys-(Ahx)-(^{68}Ga(HBED-CC)) versus 3D CT volumetric lymph node assessment in recurrent prostate cancer. *Eur J Nucl Med Mol Imaging.* 2015;42:1794-800.

17. Edge SB, Byrd DR, editors. *AJCC cancer staging manual* (7th ed). New York, NY: Springer; 2010.

18. Moltz JM, Bornemann L, Kuhnigk JM, et al. Advanced segmentation techniques for lung nodules, liver metastases, and enlarged lymph nodes in CT Scans. *IEEE Processing*. 2009;3:122-134.

19. Hijazi S, Meller B, Leitsmann C, et al. Pelvic lymph node dissection for nodal oligometastatic prostate cancer detected by ^{68}Ga-PSMA-positron emission tomography/computerized tomography. *Prostate.* 2015;75:1934-40.

20. Krohn T, Verburg FA, Pufe T, et al. ((68)Ga)PSMA-HBED uptake mimicking lymph node metastasis in coeliac ganglia: an important pitfall in clinical practice. *Eur J Nucl Med Mol Imaging.* 2015;42:210-4.

21. Christoph R, Shozo O, Philipp M, et al. ^{68}Ga-PSMA-HBED-CC ligand uptake in cervical, coeliac and sacral ganglia as an important pitfall in prostate cancer PET imaging. *J Nucl Med.* 2016;57(suppl 2):517.

22. Maurer T, Weirich G, Schottelius M, et al. Prostate-specific membrane antigen-radioguided surgery for metastatic lymph nodes in prostate cancer. *Eur Urol*. 2015;68:530-4.

23. Briganti A, Karnes RJ, Joniau S, et al. Prediction of outcome following early salvage radiotherapy among patients with biochemical recurrence after radical prostatectomy. *Eur Urol.* 2014; 66:479-86.

24. Wenger H, Weiner AB, Razmaria A, Paner GP, Eggener SE. Risk of lymph node metastases in pathological gleason score <6 prostate adenocarcinoma: Analysis of institutional and population – based databases. *Urol Oncol.* 2017;35:31.e1-31.e6.

25. van Leeuwen PJ, Stricker P, Hruby G, et al. ^{68}Ga-PSMA has a high detection rate of prostate cancer recurrence outside the prostatic fossa in patients being considered for salvage radiation treatment. *BJU Int.* 2016;117:732-9.

26. Epstein JI, Egevad L, Amin MB, Grading Committee. The 2014 International Society of Urological Pathology (ISUP) consensus conference on gleason grading of prostatic carcinoma: definition of grading patterns and proposal for a new grading system. *Am J Surg Pathol*. 2016;40:244-52.

27. Szabo Z, Mena E, Rowe SP et al., Initial Evaluation of [(18)F]DCFPyL for Prostate-Specific Membrane Antigen (PSMA)-Targeted PET Imaging of Prostate Cancer. Mol Imaging Biol. 2015 Aug;17(4):565-74. doi: 10.1007/s11307-015-0850-8.

28. Giesel FL, Hadaschik B, Cardinale J et al. F-18 labelled PSMA-1007: biodistribution, radiation dosimetry and histopathological validation of tumor lesions in prostate cancer patients. Eur J Nucl Med Mol Imaging. 2016 Nov 26.

29. Giesel FL, Kesch C, Yun J et al. 18F-PSMA-1007 PET/CT Detects Micrometastases in a Patient With Biochemically Recurrent Prostate Cancer. Clinical Genitourinary Cancer 2017, in print.

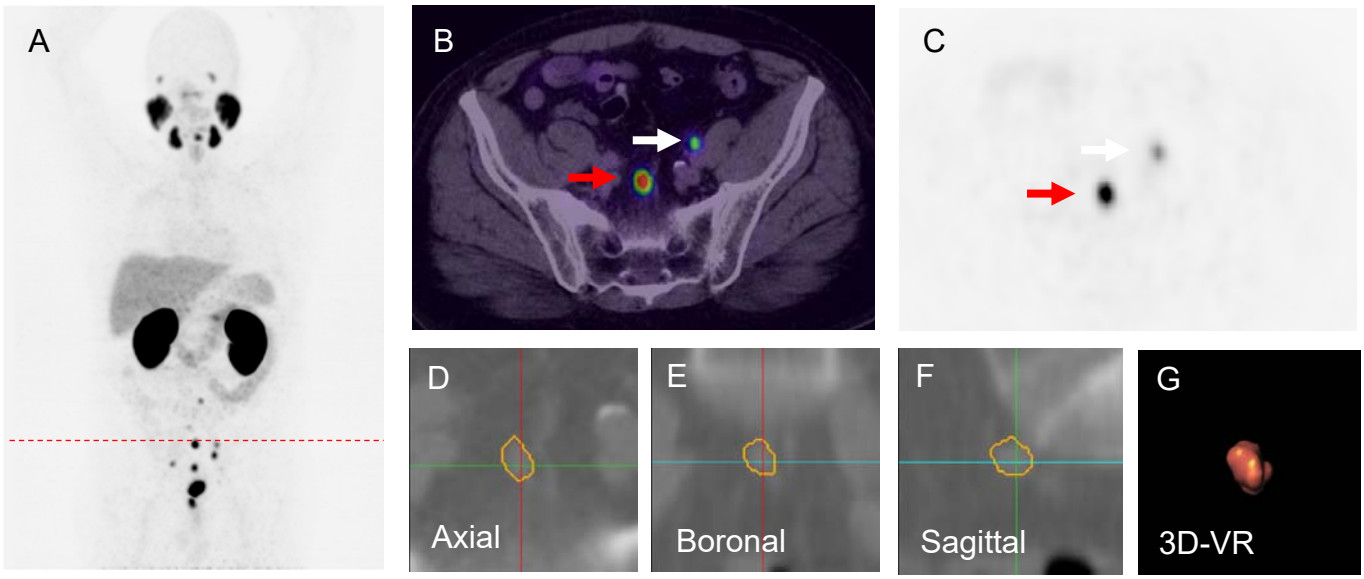

Figure 1: A 66-year-old patient with PSA relapse of 9.1 ng/mL, 5 years after radical prostatectomy (Gleason score 9, initial PSA level 69.9 ng/mL). The ^{68}Ga-PSMA PET maximum intensity projection demonstrates multiple positive nodes in the pelvic and abdominal region (a). Single axial PET/CT image (b) presents two PSMA-positive nodes (arrows). The node pointed by red arrow (c) with SUVmax 36.32 was segmented using Fraunhofer MEVIS software. The software enables automatic quantification of the dimensions based on axial (d), coronal (e) and sagittal planes (g) of CT-images (short-axis diameter 7.57 mm, long-axis diameter 11.35 mm, volume 0.5 ml). Image (g) shows 3D-volume rendering which also provided by the software.

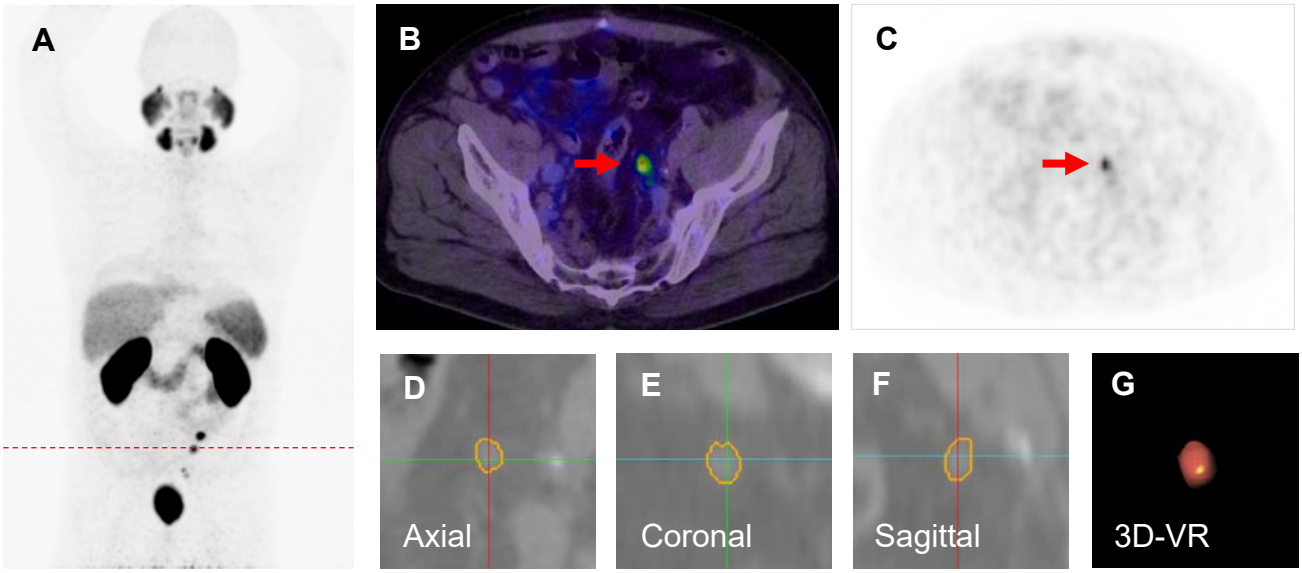

Figure 2: A 58-year-old patient with PSA relapse of 4.9 ng/mL, 9 months after prostatectomy (Gleason score 6, initial PSA 10 ng/mL). Patient presented multiple ^{68}Ga-PSMA-PET-positive nodes as shown in the PET maximum intensity projection (a). A positive node (red arrow) with PSMA uptake SUVmax 7.2 (b,c) was segmented using Fraunhofer MEVIS software. Short-axis diameter 5.93 mm, long-axis diameter 7.73 mm and volume 0.31 ml. Image (d, e, f) show the segmented lymph node on each plane and (g) the volume rendering.

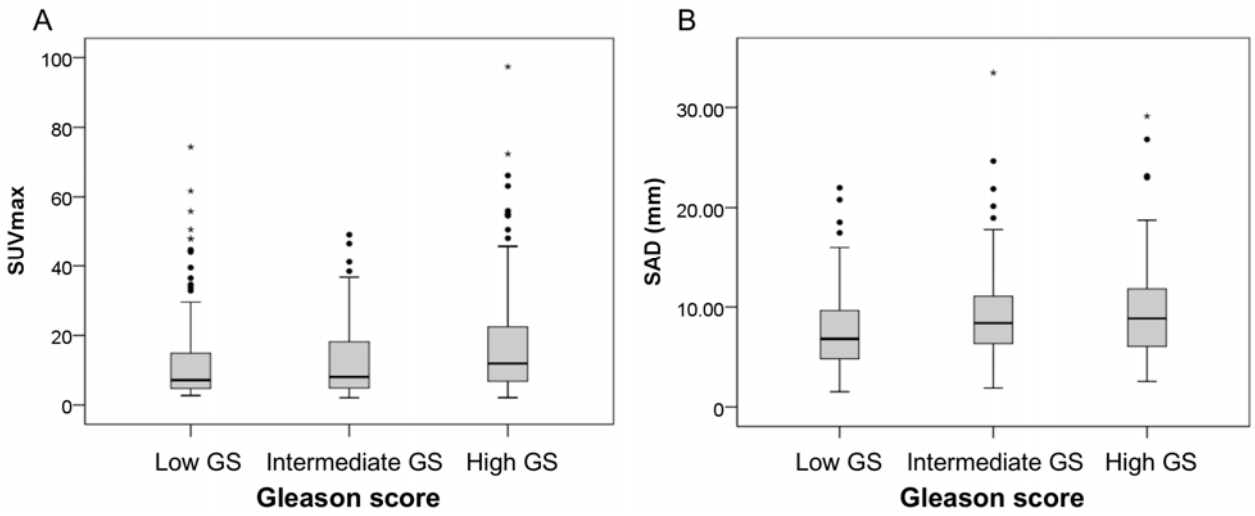

Figure 3: Uptake and morphological distribution in each risk group. (a) ^{68}Ga-PSMA ligand uptake as represented with SUV_{max} also shown an increasing trend together with risk profile.Short-axis diameter (b) of ^{68}Ga-PSMA positive lymph node presents that most metastatic lymph nodes are smaller than 10 mm, indicating that ^{68}Ga-PSMA is able to detect micrometastasis. The short-axis diameter shows a growing tendency alongside the risk profile.

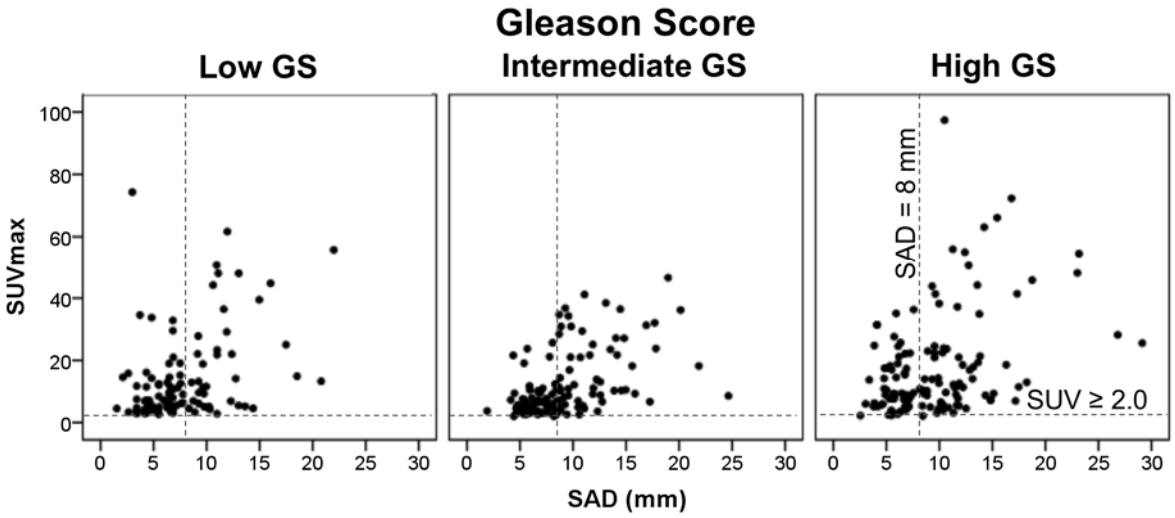

Figure 4: The relationship between SUV_{max} and short-axis diameter (SAD, mm). CT morphological cut-off was set at 8 mm and PET/CT SUV_{max} at 2.0.

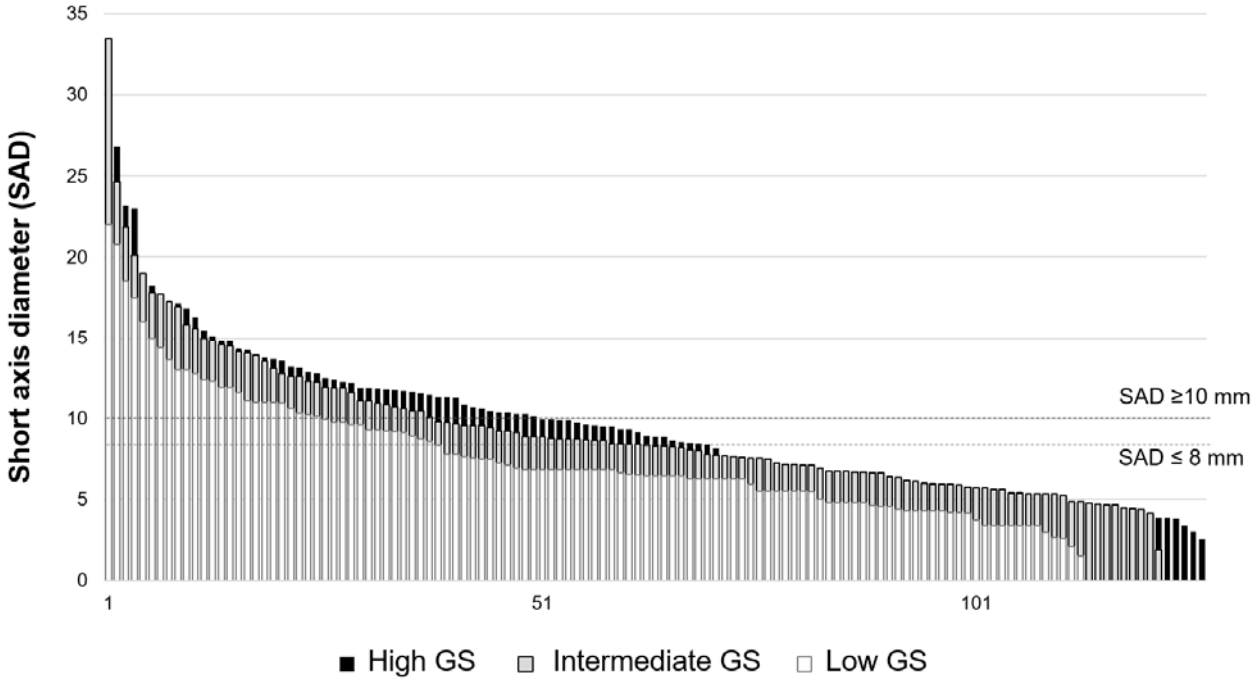

Figure 5: Morphological distribution of all 362 lymph nodes aligned to their short-axis diameter. The cut-off short-axis diameter was set to both 10 mm and 8 mm. This graph demonstrates that around two third of the PSMA-positive nodes are not sufficiently detected based on their morphologic criteria.

Patient Characteristic	*n (Range)*
Number of patients	147
Low Gleason Score Cohort	
Number of patients	51
Median age (y)	71 (59-87)
Gleason Score	6
Initial PSA (median; ng/mL)	11.3 (3.2-84.3)
Biochemical reccurrence PSA (median; ng/mL)	5.0 (0.5-41.3)
Time interval from RP to BCR (mean; months)	103
Further treatment	
Radiation therapy after RP	5
Androgen deprivation therapy during/ prior imaging	4
Unknown	20
Intermediate Gleason Score Cohort	
Number of patients	48
Median age (y)	66 (52-85)
Gleason Score	7
Initial PSA (median; ng/mL)	12.0 (3.8-252.0)
Biochemical reccurrence PSA (median; ng/mL)	5.1 (0.3-212.0)
Time interval from RP to BCR (mean; months)	56
Further treatment	
Radiation therapy after RP	20
Androgen deprivation therapy during/ prior imaging	12
Unknown	6
High Gleason Score Cohort	
Number of patients	48
Median age (y)	66 (44-80)
Gleason Score	≥8
Initial PSA (median; ng/mL)	23.5 (2-241)
Biochemical reccurrence PSA (median; ng/mL)	5.0 (0.2-293.7)
Time interval from RP to BCR (mean; months)	45
Further treatment	
Radiation therapy after RP	15
Androgen deprivation therapy during/ prior imaging	18
Unknown	8

Table 1: Patient Characteristics

Risk Profile	SUVmax			SAD (mm)			LAD (mm)			Volume (ml)		
	Mean	CI 95% Lower	CI 95% Upper	Mean	CI 95% Lower	CI 95% Upper	Mean	CI 95% Lower	CI 95% Upper	Mean	CI 95% Lower	CI 95% Upper
Low GS	13.5	10.9	16.1	7.7	6.9	8.4	11.9	11.0	12.7	1.0	0.8	1.2
Intermediate GS	12.4	9.9	14.9	9.4	8.6	10.2	13.9	12.8	14.9	1.6	1.1	2.2
High GS	17.8	15.4	20.3	9.5	8.7	10.4	14.2	13.1	15.2	1.7	1.1	2.3

Table 2: Mean SUVmax, SAD, LAD and Volume between each cohort.

Pairwise Comparisons				
Risk Profile (I*J)	p-value*			
	SUVmax	SAD	LAD	Volume
Mixed-model 3 groups	0.062	0.013*	0.023*	0.110
Low GS vs. Intermediate GS	0.797	0.011*	0.024*	0.150
Intermediate GS vs. High GS	0.031	0.953	0.801	0.540
Low GS vs. High GS	0.057	0.009*	0.012*	0.040

* The mean difference is significant at the 0.05 level

Table 3: Pairwise comparisons between each cohort